

Dispersion properties of a nanophotonic Bragg waveguide with finite aperiodic cladding

Volodymyr I. Fesenko^{1,*}, Vladimir R. Tuz^{1,2},
Oleksiy V. Shulika³, and Igor A. Sukhoivanov³

¹*Institute of Radio Astronomy of NASU, Ukraine*

²*School of Radio Physics, V.N. Karazin Kharkiv National University, Ukraine*

³*Department of Electronic Engineering and Communications, DICIS, University
of Guanajuato, Mexico*

[*v.i.fesenko@ieee.org](mailto:v.i.fesenko@ieee.org); volodymyr.i.fesenko@gmail.com

Abstract: A comprehensive analysis of guided modes of a novel type of a planar Bragg reflection waveguide which consists of a low refractive index guiding layer sandwiched between two finite aperiodic mirrors is presented. The layers in the mirrors are aperiodically arranged according to the Kolakoski substitution rule. In such a waveguide light is confined inside the core by Bragg reflection from the mirrors, while dispersion characteristics of guided modes strongly depend on aperiodicity of the cladding. Using the transfer matrix formalism bandgap conditions, dispersion characteristics and mode profiles of the guided modes of such Bragg reflection waveguide are studied.

© 2015 Optical Society of America

OCIS codes: (130.3120) Integrated optics devices; (130.5296) Photonic crystal waveguides; (230.7390) Waveguides, planar; (230.4170) Multilayers; (310.4165) Multilayer design.

References and links

1. A. J. Fox, "The grating guide – A component for integrated optics," *Proceedings of IEEE* **62**, 644–645 (1974).
2. P. Yeh, and A. Yariv, "Bragg reflection waveguides," *Opt. Commun.* **19**, 427–430 (1976).
3. P. Yeh, A. Yariv, and E. Marom, "Theory of Bragg fiber," *J. Opt. Soc. Am.* **68**, 1196–1201 (1978).
4. Qing Hu, Liu-Yang Sun, Di-Hu Xu, Yu Zhou, Ru-Wen Peng, and Mu Wang, "Tunable multimode and narrowband in a photonic quasicrystal waveguide," *J. Nanosci. Nanotechnol.* **13**, 873–877 (2013).
5. I. A. Sukhoivanov, S. O. Iakushev, O. V. Shulika, A. Díez, and M. Andrés, "Femtosecond parabolic pulse shaping in normally dispersive optical fibers," *Opt. Express* **21**, 17769–17785 (2013).
6. D. N. Chigrin, A. V. Lavrinenko, and C. S. Torres, "Nanopillars photonic crystal waveguides," *Opt. Express* **12**, 617–622 (2004).
7. A. W. Snyder, and J. D. Love, *Optical Waveguide Theory* (Chapman and Hall, London, New-York, 1983).
8. P. Russell, "Photonic crystal fibers," *Science* **299**, 358–362 (2003).
9. B. Nistad, M. W. Haakestad, and J. Skaar, "Dispersion properties of planar Bragg waveguides," *Opt. Commun.* **265**, 153–160 (2006).
10. V. I. Fesenko, V. R. Tuz, P. P. Rocha García, and I. A. Sukhoivanov, "Dispersion properties of a one-dimensional aperiodic OmniGuide structure," in *Photonic Fiber and Crystal Devices: Advances in Materials and Innovations in Device Applications VIII*, S. Yin and R. Guo, eds., Proc. SPIE **9200**, 1–7 (2014).

11. J. Li, and K. S. Chiang, "Light guidance in a photonic bandgap slab waveguide consisting of two different Bragg reflectors," *Opt. Commun.* **281**, 5797–5803 (2008).
 12. V. I. Fesenko, I. A. Sukhoivanov, S. N. Shul'ga, and J. A. Andrade-Lucio, "Propagation of electromagnetic waves in anisotropic photonic structures," in *Advances in Photonic Crystals*, Vittorio M. N. Passaro, ed. (InTech, Rijeka, 2013), pp 79–105.
 13. S. Dasgupta, A. Ghatak, and B. P. Pal, "Analysis of Bragg reflection waveguides with finite cladding: An accurate matrix method formulation," *Opt. Commun.* **279**, 83–88 (2007).
 14. B. R. West, and A. S. Helmy, "Properties of the quarter-wave Bragg reflection waveguide: Theory," *J. Opt. Soc. Am. B* **23**, 1207–1220 (2006).
 15. Yu Li, Yanping Xi, Xun Li, and Wei-Ping Huang, "A single-mode laser based on asymmetric Bragg reflection waveguides," *Opt. Express* **17**, 11179–11186 (2009).
 16. Bishnu P. Pal, Somnath Ghosh, R. K. Varshney, Sonali Dasgupta, Ajoy Ghatak, "Loss and dispersion tailoring in 1D photonics band gap Bragg reflection waveguides: Finite chirped claddings as a design tool," *Opt. Quant. Electron.* **39**, 983–993 (2007).
 17. Y. Fink, J. N. Winn, S. Fan, C. Chen, J. Michel, J. D. Joannopoulos, and E. L. Thomas, "A dielectric omnidirectional reflector," *Science* **282**, 1679–1682 (1998).
 18. M. Ibanescu, Y. Fink, S. Fan, E. L. Thomas, and J. D. Joannopoulos, "An all-dielectric coaxial waveguide," *Science* **289**, 415–419 (2000).
 19. S. G. Johnson, M. Ibanescu, M. Skorobogatiy, O. Weisberg, T. D. Engeness, M. Soljačić, S. A. Jacobs, J. D. Joannopoulos, and Y. Fink, "Breaking the glass ceiling: hollow OmniGuide fibers," in *Photonic Bandgap Materials and Devices*, A. Adibi, A. Scherer and Shawn-Yu Lin, eds., *Proc. SPIE* **4655**, 1-15 (2002).
 20. D. Lusk, I. Abdulhalim, and F. Placido, "Omnidirectional reflection from Fibonacci quasi-periodic one-dimensional photonic crystal," *Opt. Commun.* **198**, 273–279 (2001).
 21. F. Qiu, R. W. Peng, X. Q. Huang, X. F. Hu, Mu Wang, A. Hu, S. S. Jiang, and D. Feng, "Omnidirectional reflection of electromagnetic waves on Thue-Morse dielectric multilayers," *Europhys. Lett.* **68**, 658 (2004).
 22. A. Barriuso, J. Monzón, L. Sánchez-Soto, and A. Felipe, "Comparing omnidirectional reflection from periodic and quasiperiodic one-dimensional photonic crystals," *Opt. Express* **13**, 3913–3920 (2005).
 23. V. I. Fesenko, V. R. Tuz, and I. A. Sukhoivanov, "Optical characterization of the aperiodic multilayered anisotropic structure based on Kolakoski sequence," in *Integrated Optics: Physics and Simulations*, P. Cheben, J. Ctyroký and I. Molina-Fernandez, eds., *Proc. SPIE* **8781**, 87811C-1–87811C-7 (2013).
 24. V. I. Fesenko, "Aperiodic birefringent photonic structures based on Kolakoski sequence," *Waves Rand. Complex* **24**, 174–190 (2014).
 25. V. I. Fesenko, "Omnidirectional reflection from generalized Kolakoski multilayers," *Prog. Electromagn. Res. M* **41**, 33–41 (2015).
 26. V. R. Tuz, "Optical properties of a quasiperiodic generalized Fibonacci structure of chiral and material layers," *J. Opt. Soc. Am. B* **26**, 627–632 (2009).
 27. V. R. Tuz and V. B. Kazanskiy "Electromagnetic scattering by a quasiperiodic generalized multilayer Fibonacci structure with grates of magnetodielectric bars," *Waves Rand. Complex* **19**, 501–508 (2009).
 28. V. R. Tuz, "A peculiarity of localized mode transfiguration of a Cantor-like chiral multilayer," *J. Opt. A: Pure Appl. Opt.* **11**, 125103 (2009).
 29. W. Kolakoski, "Self generating runs, Problem 5304," *Amer. Math. Monthly* **72**, 674 (1965).
 30. B. Sing, "Kolakoski sequences – an example of aperiodic order," *J. Non-Cryst. Solids* **334**, 100–104 (2004).
 31. J.-S. I, Y. Park, and H. Jeon, "One-dimensional photonic crystal waveguide: A frame for photonic integrated circuits," *J. Korean Phys. Soc.* **39**, 994–997 (2001).
 32. J.-S. I, Y. Park, and H. Jeon, "Optimal design for one-dimensional photonic crystal waveguide," *J. Light. Tech.* **22**, 509–513 (2004).
 33. G. P. Agrawal, *Nonlinear Fiber Optics. Third Edition* (Academic Press, San Diego, 2001).
 34. J. Li, and K. S. Chiang, "Guided modes of one-dimensional photonic bandgap waveguides," *J. Opt. Soc. Am. A* **24**, 1942–1950 (2007).
 35. F. Villa, and J. Gaspar-Armenta, "Photonic crystal to photonic crystal surface modes: narrow-bandpass filters," *Opt. Express* **12**, 2338–2355 (2004).
-

1. Introduction

Bragg reflection waveguides [1, 2] are photonic structures, designed to guide light within a core layer surrounded by a special composite cladding whose effective refractive index can be either lower or higher than the core one. The cladding can have different configurations, e.g. it can be designed as a multilayer stack of periodically arranged dielectric layers (slab waveguides) [1, 2], coaxial layers having alternated high and low refractive indices (Bragg fibers) [3, 4], arrays of holes in a single-material dielectric film or fiber [5], systems of dielectric pillars [6], etc. In all mentioned designs, unlike the conventional high-index guiding waveguides based on the total internal reflection [7], principal characteristics of Bragg reflection waveguides are influenced by periodicity in their cladding constituents. Indeed, the periodicity in constituents leads to formation of photonic bandgaps in the spectra of Bragg mirrors resulting in light confinement within a core layer. Such photonic bandgap guidance brings several attractive features to the waveguide characteristics [8], in particular, since most of light is guided inside a low-index core (which can even be an air channel), losses and nonlinear effects can be significantly suppressed. Moreover, the mode area, mode profile and dispersion properties of Bragg reflection waveguides can be optimized providing specific choice of constituents and cladding configuration (e.g. utilization of chirping [9] or aperiodic [10] designs for the Bragg mirrors). The interest to the mentioned unique features of Bragg reflection waveguides arises sufficiently in recent years due to advances in the deposition and crystal growth technologies, which made possible the fabrication of waveguides with complicate designs assuring an appropriate quality.

First of all, as an ideal model, a Bragg reflection waveguide made of a low-index layer sandwiched between two identical *semi-infinite* one-dimensional Bragg mirrors is considered in [2]. In such a system the semi-infinite configuration of mirrors guarantees existence of the total reflection within complete photonic bandgaps that provides perfect light guiding inside the core. From the theoretical standpoint, an efficient mathematical method based on the Bloch wave formulation is applied to analyze and tailor the propagation characteristics of modes in such waveguide. However, in designs of practical systems the multilayer structure of cladding definitely has a *finite* extent which requires taking into account an energy leakage from the waveguide through its imperfect mirrors that is out of scope of the Bloch wave formulation related to the infinitely extended periodic medium.

In order to consider a more realistic model of Bragg reflection waveguides with a finite extent of multilayer mirrors among other purely numerical simulations based on propagation methods [11, 12], in the one-dimensional case the transfer matrix formalism [13] is widely used which assumes matching the boundary conditions at interfaces between high- and low-index layers and enables one to derive an analytic solution on this basis. Although the latter method is only applicable for simple configurations of Bragg reflection waveguides, in many cases it allows to offer deep physical insight into the problem. The solution for a planar Bragg waveguide can be derived in the form of the TE and TM modes considered separately, with two sets of 2×2 transfer matrices, while the cylindrical Bragg fiber case requires 4×4 matrices in general. Nevertheless, since most of characteristics of planar Bragg waveguides are similar to those of cylindrical Bragg fibers, it is well known that results obtained with the transfer matrix method for one-dimensional planar systems are also applicable for prediction of optical features of fibers without re-solving the problem for the cylindrical geometry.

In the search for improved features of Bragg reflection waveguides, aside from a standard configuration of the waveguide with a periodic quarter-wave cladding [14],

it has been proposed and studied a number of designs among which we distinguish particular configurations consisted of a guiding layer placed between two different Bragg reflectors [11, 15], mirrors with a periodicity defect [9] and chirped claddings [9, 16]. Thus it is shown that in the case of a waveguide with two different Bragg reflectors two distinct sets of bandgaps can be obtained and the waves guided along the waveguide appear to be inside their overlapped bandgaps. By manipulating two sets of bandgaps independently, the flexibility in the control of transmission characteristics of the guided modes can be enhanced significantly. Furthermore by introducing a defect inside the mirror's structure it is possible to shift the zero-dispersion point toward longer wavelengths.

At the same time the most promising technique is seen to be in the use of the omnidirectional reflection feature which is available in multilayer photonic structures [17]. In [18, 19] a particular design of Bragg reflection waveguides utilizing omnidirectional reflection is referred to "OmniGuide" fibers. Such omnidirectional reflection in the waveguide cladding results in strong resemblances of OmniGuide fiber features to those ones of the convenient hollow metallic waveguides, confining a set of guided modes almost entirely within the hollow core with similar field patterns and dispersion characteristics.

Here we propose a way for the integration of these mentioned improvements within a single system by utilization of a deterministically *aperiodic* design in the cladding. It is no doubt that a deterministically aperiodic multilayer system can be considered as a periodic one having plural defects and thus aperiodic configuration gives an opportunity to customize dispersion characteristics of the waveguide. Another key point is that aperiodic multilayers possess a much more complex structure in the reciprocal space than periodic ones. It results in presence of several omnidirectional photonic bandgaps within a period of the reciprocal space of aperiodic systems [20, 21, 22].

From our previous studies [23, 24, 25] it is found that deterministically aperiodic multilayers constructed according to the Kolakoski generation rules demonstrate pronounced omnidirectional reflectance and have completely transparent states in the transmission spectra which are important for achieving sufficient waveguide modes filtering. Therefore, in this study, we introduce an extra degree of freedom for optimizing Bragg reflection waveguides through utilization of an aperiodically layered cladding. Our goal here is to study the dispersion characteristics providing the mode classification of a planar waveguide system whose mirrors are made from dielectric layers arranged according to the mentioned Kolakoski generation rules. The solution for both TE and TM modes is constructed using the transfer matrix formalism [26, 27, 28].

2. Theoretical Description

2.1. Aperiodic Bragg Reflection Waveguide Configuration

Further we consider a Bragg reflection waveguide made of low-index core layer sandwiched between two identical aperiodic one-dimensional mirrors formed by stacking together two different materials Ψ and Υ according to the Kolakoski $K(p, q)$ generation scheme as it is shown in Fig. 1a.

The generation rule w of the Kolakoski sequence is similar to those ones of the Fibonacci or Thue-Morse sequences and can be based on two symbols substitution. Namely the sequence $K(p, q)$ can be obtained by starting with p as a seed and iterating the following two substitutions:

$$w_0 : \begin{array}{l} q \rightarrow p^q \\ p \rightarrow p^p \end{array} \quad \text{and} \quad w_1 : \begin{array}{l} q \rightarrow q^q \\ p \rightarrow q^p \end{array} \quad (1)$$

where w_0 and w_1 can be any string of letters p and q ; p^q denotes a run of p q 's, i.e.,

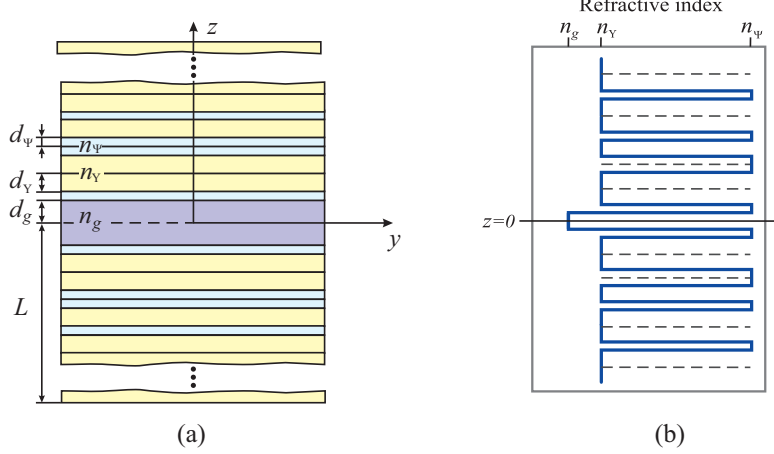


Fig. 1. (a) The schematic of a Bragg reflection waveguide with aperiodic mirrors arranged according to the Kolakoski $K(1,2)$ substitutional rules; (b) index profile of the structure.

$p^q = p \dots p$ (q times). Extra information about generation rules of the Kolakoski sequence, its general properties and configuration of different multilayers based on the Kolakoski generation scheme can be found in Refs. [29, 30] and Refs. [23, 24, 25], respectively. In this paper the number of generation stage of the sequence is defined as σ .

The structure under study is infinite along x -axis, so $\partial/\partial x = 0$. Besides, the refractive index profile of the waveguide structure varies only along z -axis and it is invariant in other directions (see, Fig. 1b). In this configuration the middle of the core is assumed to be at the line $z = 0$. We suppose that both mirrors consist of a finite number N of the constitutive layers ($\sigma < \infty$). Also it is further assumed that the letters Ψ and Υ denote two different layers with thicknesses d_Ψ , d_Υ and refractive indices n_Ψ , n_Υ , respectively. The guiding layer has thickness $2d_g$ and refractive index n_g . The total thickness of the structure under study is $2L$. In general case, the external medium outside the layered system $z < -L$ and $z > L$ is homogeneous, isotropic and can have either high or low refractive index, however, in this paper we assume that the waveguide is surrounded by air with $n_0 = 1$.

In the chosen structure configuration, each guided mode propagates along y -axis with its own propagation constant β . In our study we analyze the propagation of both TE waves and TM waves with field components $\vec{E} = \{E_x, 0, 0\}$, $\vec{H} = \{0, H_y, H_z\}$ and $\vec{E} = \{0, E_y, E_z\}$, $\vec{H} = \{H_x, 0, 0\}$, respectively. Note that in the case of the practical Bragg reflection waveguides with finite number of layers in the mirrors, the light propagation is accompanied by some attenuation that appears as a result of the energy leakage through imperfect mirrors, which is consistently taken into consideration within our model.

2.2. Transfer Matrix Description

Key task here is a definition of dispersion fields of the finite aperiodic sequence of alternating two different isotropic layers. The plane monochromatic waves of TE ($\vec{E}^{\text{TE}} \parallel \vec{x}_0$) and TM ($\vec{H}^{\text{TM}} \parallel \vec{x}_0$) polarizations can be defined in a particular j -th layer ($j =$

1, 2, ..., N) of the sequence in the form

$$\begin{Bmatrix} \vec{E}_j^{\text{TE}} \\ \vec{H}_j^{\text{TM}} \end{Bmatrix} = \vec{x}_0 \begin{Bmatrix} 1/\sqrt{Y_j^{\text{TE}}} \\ \sqrt{Y_j^{\text{TM}}} \end{Bmatrix} u_j(z) \exp[-i(\omega t - \beta y)], \quad (2)$$

where

$$u_j(z) = a_j \exp(ik_{zj}z) + b_j \exp(-ik_{zj}z), \quad (3)$$

and a_j and b_j are the field amplitudes, $Y_j^{\text{TE}} = k_{zj}/k_0\mu_j$ and $Y_j^{\text{TM}} = k_0\varepsilon_j/k_{zj}$ are the wave admittances, $k_0 = \omega/c$ is the wavenumber in free space, and k_{zj} is the transverse wavenumber which takes on discrete values in each slab and can be written as

$$k_{zj} = (k_0^2 n_j^2 - \beta^2)^{1/2} = k_0 (n_j^2 - n_{eff}^2)^{1/2}. \quad (4)$$

Here $n_{eff} = \beta/k_0$ is introduced as the effective refractive index of the guided mode, n_j takes on values n_g for the core layer, and n_Ψ and n_Y for the Ψ and Y cladding layers, respectively.

The field amplitudes for the structure input and output are evaluated as [26, 27, 28]

$$\begin{bmatrix} a_0 \\ b_0 \end{bmatrix} = \mathbf{T}_\Sigma \begin{bmatrix} a_N \\ b_N \end{bmatrix} = \left(\underbrace{\mathbf{T}_\Psi \mathbf{T}_Y \mathbf{T}_Y \mathbf{T}_\Psi \mathbf{T}_Y \dots}_N \right) \begin{bmatrix} a_N \\ b_N \end{bmatrix}, \quad (5)$$

where the total transfer matrix \mathbf{T}_Σ is obtained by multiplying in the appropriate order the matrices corresponding to each layer in the structure.

The matrices \mathbf{T}_Ψ and \mathbf{T}_Y are the particular transfer matrices of rank 2 of the Ψ and Y layers in cladding with their corresponding thicknesses d_Ψ and d_Y . They are

$$\mathbf{T}_\Psi = \mathbf{T}_{01} \mathbf{P}_1(d_\Psi) \mathbf{T}_{10}, \quad \mathbf{T}_Y = \mathbf{T}_{02} \mathbf{P}_2(d_Y) \mathbf{T}_{20}, \quad (6)$$

where \mathbf{T}_{0j} and \mathbf{T}_{j0} ($j = 1, 2$) are the transfer matrices of the layer interfaces with outer half-spaces, and $\mathbf{P}_j(d)$ are the propagation matrices through the corresponding layer. The elements of the matrices \mathbf{T}_{0j} and \mathbf{T}_{j0} are determined by solving the boundary-value problem related to the field components (2):

$$\mathbf{T}_{pv} = \frac{1}{2\sqrt{Y_p Y_v}} \begin{bmatrix} Y_p + Y_v & \pm(Y_p - Y_v) \\ \pm(Y_p - Y_v) & Y_p + Y_v \end{bmatrix}, \quad \mathbf{P}_j(d) = \begin{bmatrix} \exp(-ik_{zj}d) & 0 \\ 0 & \exp(ik_{zj}d) \end{bmatrix}, \quad (7)$$

where the upper sign ‘+’ relates to the TE wave, while the lower sign ‘-’ relates to the TM wave.

Finally, the reflection coefficient of the layer stack is determined by the expression

$$R = (b_0/a_0)|_{b_N=0} = -t_{21}/t_{22}, \quad (8)$$

where t_{mn} are the elements of the total transfer matrix \mathbf{T}_Σ .

2.3. Dispersion Equation for Guided Modes

As Bragg mirrors on both sides of the waveguide core layer are the same (i.e. the Bragg reflection waveguide is symmetrical about the z -axis, $n(-z) = n(z)$), the equations for waves travelling back and forth inside the channel can be joined on the boundaries $z = d_g$ and $z = -d_g$ into the next system

$$\begin{cases} a_0 \exp[-ik_{zg}d_g] = Rb_0 \exp[ik_{zg}d_g], \\ b_0 \exp[-ik_{zg}d_g] = Ra_0 \exp[ik_{zg}d_g], \end{cases} \quad (9)$$

from which the relation between amplitudes can be found

$$b_0 = a_0 R \exp[2ik_{zg}d_g]. \quad (10)$$

Eliminating amplitudes a_0 and b_0 from system (9) the *dispersion* equation for the guided modes of the Bragg reflection waveguide is obtained as

$$1 - R^2 \exp \left[4ik_0 d_g \sqrt{n_g^2 - n_{eff}^2} \right] = 0. \quad (11)$$

This equation is further solved numerically to find out a function of the propagation constant β versus frequency ω . Remarkably, even in the case when constitutive materials of layers in the core and cladding are considered to be without intrinsic losses, for a finite number of these layers N in the multilayer system, solutions of the dispersion equation (11) appear in the field of complex numbers β since there is an inevitable energy leakage through the outermost layers. Thus, the resulting propagation constant is sought in the complex form as $\beta = \beta' + i\beta''$.

In a semi-infinite periodic structure without intrinsic losses in its constituents, the propagation constant β takes either purely real ($\beta'' = 0$) or purely imaginary ($\beta' = 0$) values [2], where the real β corresponds to propagating waves. In the case of structure with a finite number of layers in the cladding, the roots of the dispersion equation are always complex numbers, nevertheless in order to provide the wave propagation, the imaginary part of β must be small enough. As it was demonstrated in [14], β'' becomes to be negligibly small for the number of cladding's layers more then $N = 24$ for the chosen structure parameters confirming that losses reach a value lower than 10^{-4} dB/cm in their case. Thus, in our consideration the number of layers in the cladding is defined in such a way to satisfy the criterion of smallness of the imaginary part of β when classifying waveguide modes. All other solutions are interpreted as those that belong to leaky waves and therefore are discarded from our consideration.

Furthermore, for the symmetric waveguides all guided modes can be divided onto symmetric and anti-symmetric ones. Without loss of generality, the overall field amplitude in the middle line of the core can be reduced to unity or zero for symmetric and anti-symmetric modes, respectively. Then the field in the core can be normalized by setting $a_0 = 1/2$ and $b_0 = \pm 1/2$, where the upper sign '+' is related to symmetric modes, while the lower sign '-' is related to anti-symmetric ones, respectively.

3. Numerical Results: Solution Analysis

3.1. Spectral Properties and Dispersion Diagrams

For a comparative study we further consider two different configurations of a Bragg reflection waveguide. The first configuration is a waveguide with a typical periodic cladding. In this case we repeat the results of [31] in order to verify the method of solution and comply the succession. In the second configuration the cladding is considered to be an aperiodic structure arranged according to $K(1,2)$ generation scheme. Thus, in both configurations we study a waveguide having an air core layer with thickness $2d_g = (2/3)(d_\Psi + d_\Upsilon)$ and refractive index $n_g = 1.0$. The air guiding layer is sandwiched between two identical one-dimensional photonic structures which generally reflect light back over a bounded range of angles. Nevertheless, in the particular case of existing of the omnidirectional reflection, the angular range is complete [17]. As constituents for cladding we consider combination of layers made of GaAs and oxidized AlAs, whose refractive indices at the wavelength of $1 \mu\text{m}$ are $n_\Psi = 3.50$ and $n_\Upsilon = 1.56$, respectively. The thickness ratio is defined to be $d_\Psi : d_\Upsilon = 1 : 2$. Note that similar results can be

obtained by choosing alternation of layers made of Si and SiO₂, whose refractive indices at the wavelength of 1 μm are $n_\Psi = 3.56$ and $n_\Upsilon = 1.46$, respectively. This pair of the cladding's materials will be further used for the chromatic dispersion calculation.

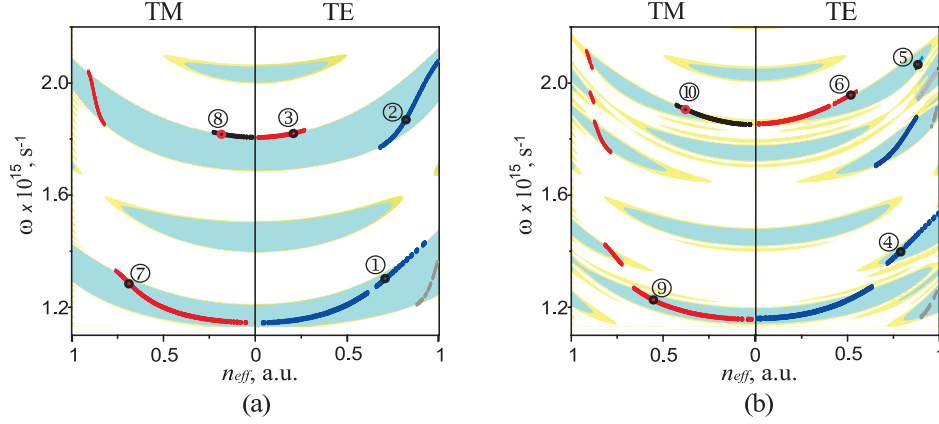


Fig. 2. The band diagrams and dispersion curves for TM and TE waves in the Bragg reflection waveguide with (a) periodic cladding and (b) aperiodic cladding. The colored areas correspond to bandgaps with level of reflection $|R| > 0.9$. The different colors of the dispersion curves correspond to different values of the mode index m : blue curves correspond to $m = 0$, red curves correspond to $m = 1$, and black curves correspond to $m = 2$. The gray lines represent modes with $m = -1$; $N = 24$.

As a typical example in Fig. 2 we demonstrate the band diagrams and dispersion curves which are calculated for two mentioned particular waveguide's cladding configurations. These results are obtained for the same number N and material parameters n_Ψ and n_Υ of the constitutive layers for both cladding configurations. Here the regions colored in light yellow indicate the photonic bands of the Bragg mirrors where the level of reflection lies within the range $0.9 < |R| < 0.999$ for both TE and TM waves. Also the regions colored in light blue correspond to the level of reflection $|R| \geq 0.999$ which can be identified as bandgaps. The middle line $n_{eff} = 0$ divides band diagrams onto two parts, where the left side represents features of TM waves, while the right one represents features of TE waves.

In the case of periodic cladding (Fig. 2a), in the band diagram on either side of the line $n_{eff} = 0$ there is a set of n disjoint bands where the level of reflection reaches very high values ($R \geq 0.999$). They are centered around frequencies $\omega_v = v\pi c / (n_\Psi d_\Psi + n_\Upsilon d_\Upsilon)$, where ω_v is a central frequency of the corresponding band and v is the band order (in the presented fragment of the band diagram v acquires values 4, 5, 6 and 7). At the same time the band diagram of the system with an aperiodic arrangement is more complicated (Fig. 2b). Thus, on both sides of the line $n_{eff} = 0$ there is a set of bandgaps ($|R| \geq 0.999$) with the same central frequency ω_v as for the periodic structure. But all the bands get narrower for both TE and TM waves. Besides, as value of n_{eff} moves towards 1 some additional high-reflectance bands appear for both TE and TM waves.

Furthermore in both structure configurations the coverage areas of bands related to TM waves are smaller than those ones of TE waves, which is consistent with other observations on the reflection bandwidths of the two polarizations (see, for instance [21, 25]). In fact, the bands of TM waves appear to be totally covered by the corresponding bands

of TE waves. Therefore, it is enough to provide analysis of omnidirectional reflection only on the basis of bands characteristics of TM waves.

In particular, in our previous investigations [10, 25] it is demonstrated that multilayer structures, arranged according to the classical and generalized Kolakoski self-generation schemes, can acquire several overall omnidirectional reflection bands. The omnidirectional reflection is achieved by accurate adjusting material parameters and geometrical structure of the distributed Bragg reflectors, such as refractive indices ratio $r = n_Y/n_\Psi$ and thicknesses of the constitutive layers d_Ψ and d_Y . Particularly, the refractive indices ratio r should be as high as possible, but for practical structures this ratio can be limited by availability of materials that are used in the integrated optic circuits. Therefore the thicknesses of the layers also should be accurately tuned, namely, the individual layer thickness of a surrounded Bragg reflector must be chosen exactly to be one quarter of an operating wavelength [32]. In our case it is obvious that for the structure under study, these criteria are not met and, therefore, there is not any omnidirectional reflection band for both structure configurations.

On the other hand Fig. 2 presents information about calculated dispersion curves for both configurations of a Bragg reflection waveguide having periodic or aperiodic cladding. The waveguide modes are indicated by a set of colored points. All these modes appear only within the gaps where the level of reflection riches high values ($|R| \geq 0.999$). Within the neighbor bandgaps dispersion curves can have the same mode index m , while they disappear outside the range of bandgaps. In fact, these curves have discontinuities at the bandgap edges at which there is a mode cutoff. Moreover, in the aperiodic configuration the dispersion curves have more cutoff points for each mode than those of periodic one. It means that Bragg reflection waveguides with aperiodic cladding are easier to be optimized than that ones with periodic cladding to support propagation of desired modes only. Thus, an aperiodic configuration of cladding of Bragg reflection waveguide can give rise to exceptionally strong mode selection and tuning the polarization-discrimination effects.

3.2. Mode-Field Patterns and Confinement Factor

A guided mode in the Bragg reflection waveguide can be considered as a plane wave travelling back and forth in the core, forming a standing wave pattern. Figs. 3 and 4 depict the mode-field patterns for a number of TE_m and TM_m modes with the lowest index m . As before in these figures both periodic and aperiodic configurations of cladding are presented. The numbers in circles from 1 to 10 are ranged according to the marked points presented on the dispersion curves in Fig. 2. The patterns are plotted after applying normalization of the field magnitude on its maximal value within the core. The fractional power in the guiding layer is known as the energy confinement factor Γ that is defined in the form [32, 33]

$$\Gamma = \frac{\int_{-d_g}^{d_g} |\eta|^2 dz}{\int_{-L}^L |\eta|^2 dz}, \quad (12)$$

where η is related to field components E_x and H_x for TE and TM waves, respectively. As known in a conventional slab waveguide, with $n_g > n_{clad}$, the field decays exponentially in the cladding as waves propagate away from the core. However, in a planar Bragg reflection waveguide the field acquires some oscillations inside the layered system of mirrors for both the periodic and aperiodic configurations. The magnitude of these oscillations decays monotonically away from the guiding layer as it is depicted in

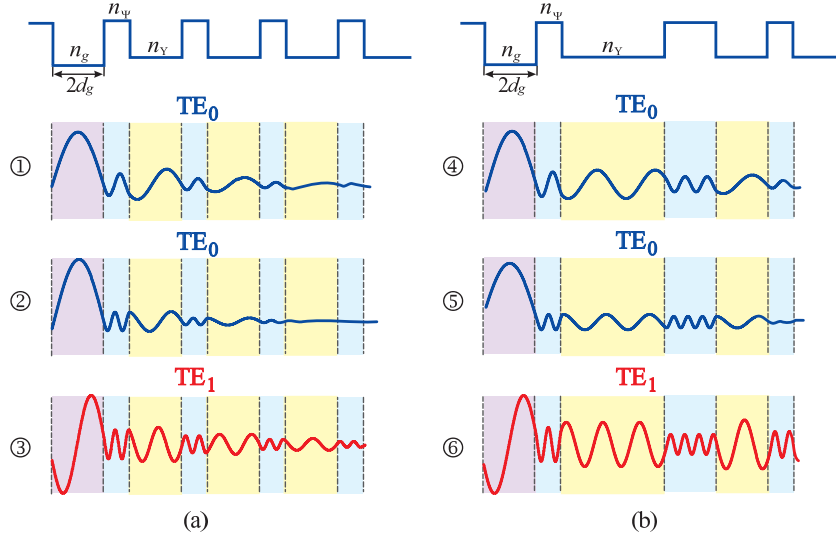


Fig. 3. Electric-field patterns related to the E_x component of the field for TE_m modes. The refractive index profile of the corresponding waveguide is presented on the top of figure. The confinement factor is: (1) $\Gamma = 0.77$; (2) $\Gamma = 0.92$; (3) $\Gamma = 0.22$; (4) $\Gamma = 0.73$; (5) $\Gamma = 0.87$; (6) $\Gamma = 0.35$.

Figs. 3 and 4. Besides, as it is described in [11, 34], for Bragg reflection waveguides with periodic cladding, the band order ν defines a number of zero crossings in every pair of the constitutive layers of the cladding. For an aperiodic configuration of cladding this condition is not satisfied, because some of the constitutive layers appear to be repeated in a row producing a layer with a doubled thickness. As a result, there are ν , $\nu + 2$ or $\nu + 4$ zero crossings in every pair of the structure layers. At the same time, by analogy with a conventional slab waveguide [7], the mode index m specifies an integer number of the field's zeros in the guiding layer. On the other hand an integer number of the field peaks in the guiding layer can be defined as $m + 1$. In this notation, the even integer numbers correspond to the symmetric modes, while the odd ones correspond to the anti-symmetric modes.

The lowest mode order of a conventional waveguide is usually $m = 0$. However as it is shown in [34], when the thickness of the guiding layer satisfies the condition

$$d_g \leq d_2, \quad (13)$$

where d_2 is the thickness of the second layer of the cladding, a few modes with negative integer number $m = -1$ may emerge. In the considered case $d_2 = 2d_1 = 4d_g$ and $d_2 = d_1 = 2d_g$ for aperiodic and periodic cladding, respectively, so condition (13) is satisfied. The dispersion curves of the TE_{-1} mode are distinguished in Fig. 2 by grey color. Both the number of field peaks and zero crossings within the guiding layer become to be zero for these modes. In fact, these modes can be interpreted as surface modes whose energy is confined around the interface of two coupled periodic/aperiodic structures [35].

The confinement factor of several low-order modes is shown in Fig. 5. From these curves it follows, that the confinement factor of both TM_m and TE_m modes is lower for aperiodic structure as compared to the periodic one, so energy leakage from the aperiodic cladding is greater. This is due to the fact that bandgaps are narrower in the

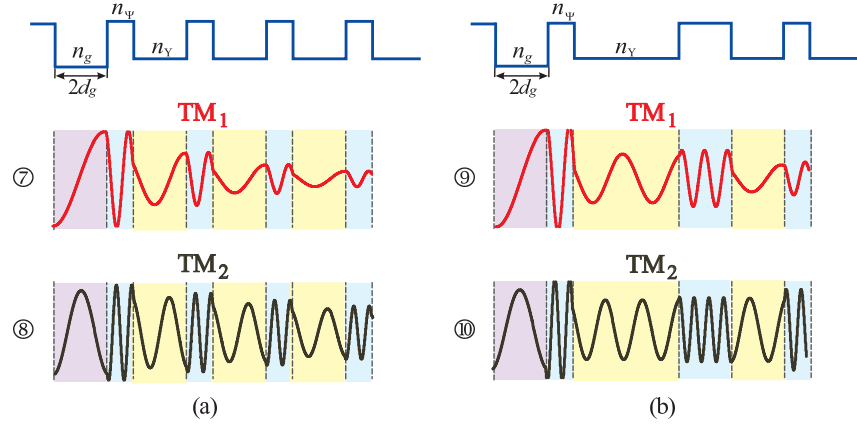


Fig. 4. Magnetic-field patterns related to the H_x component of the field for TM_m modes. The refractive index profile of the corresponding waveguide is presented on the top of figure. The confinement factor is: (7) $\Gamma = 0.3$; (8) $\Gamma = 0.14$; (9) $\Gamma = 0.23$; (10) $\Gamma < 0.1$.

aperiodic systems. Although the confinement factor of the modes is not high enough, the light energy is confined strongly within the first few pairs of the constitutive layers of the cladding as it is depicted in Figs. 3 and 4.

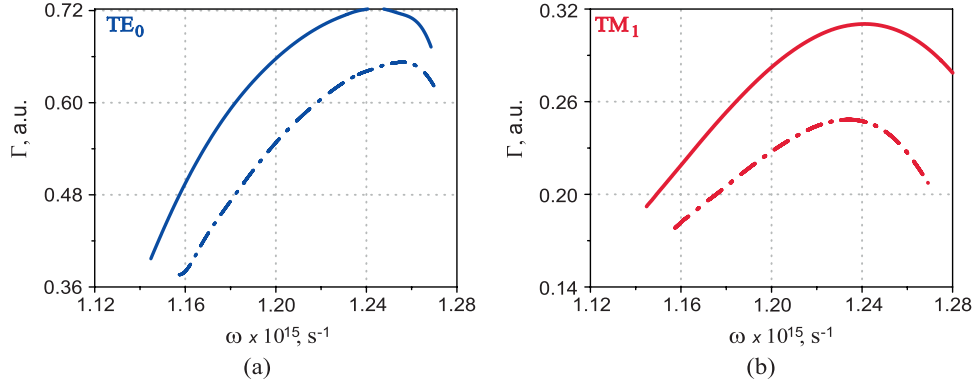


Fig. 5. Variation of the confinement factor Γ versus frequency ω for several guided modes: (a) TE_0 modes; (b) TM_1 modes. Here solid curves correspond to periodic cladding, while dashed curves correspond to aperiodic cladding. In all cases $N = 10$.

Moreover, the confinement factor reduces, but remains finite, when the dispersion curve approaches the band edges where there is a mode cutoff. As a result, the confinement factor attains some maximum between these two cutoff points. At the same time the confinement factor of each mode is higher in the bandgap with the highest band order ν . This is due to the fact that the effective refractive index n_{eff} (which lies between 0 and n_g) acquires its maximal value in this case. Note, in Bragg reflection waveguides a larger confinement factor always corresponds to a larger value of $n_{eff} = \beta/k_0$, because the normalized propagation constant $\tilde{\beta} = (n_{eff}^2 - n_Y^2)/(n_\Psi^2 - n_Y^2)$ increases as n_{eff} rises

resulting in the mode field concentrating inside the core.

We should note, that in conventional waveguides based on the total internal reflection [7] there is only a *single* cutoff point for each guided mode and Γ gradually approaches to 1 when operating frequency increases. Unfortunately it is accompanied by increasing in the number of guided modes that become to be propagating at this frequency. As a result, in such waveguides with discrete spectra of guided modes, a confinement factor of the fundamental mode approaches to its maximal value in the region where high order modes also exist. In contrast to a conventional waveguide, as it was demonstrated in previous section, Bragg reflection waveguides and especially Bragg reflection waveguides with aperiodic cladding are characterized by more complicated spectra of guided modes. So that, in a certain frequency range, they can support a single-mode regime with high degree of confinement of the guided mode not only for the fundamental mode but also for other high-order ones.

3.3. Chromatic Dispersion

Chromatic dispersion, which is manifested by the frequency dependence of the phase velocity and group velocity on refractive indexes of waveguide constituents (material dispersion) as well as its geometrical parameters (waveguide dispersion), is a significant factor in design of the photonic devices. In the field of optical waveguides, a dispersion parameter D is commonly used for accounting effects of the chromatic dispersion. The dispersion parameter D may be calculated as [33]:

$$D = -\frac{\omega^2}{2\pi c} \beta'_2, \quad (14)$$

where $\beta'_2 = d^2\beta'/d\omega^2$ is the group velocity dispersion which is responsible for pulse broadening.

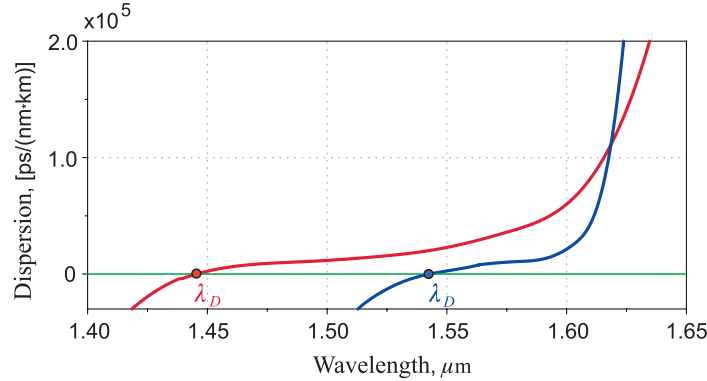


Fig. 6. Dispersion of the fundamental TE₀ mode. Red and blue curves correspond to two particular configurations of a Bragg reflection waveguide with periodic and aperiodic cladding, respectively. Green line represents level $D = 0$ [ps/(nm · km)].

The dispersion curves of the fundamental TE₀ mode for both periodic and aperiodic configurations of a Bragg reflection waveguide are presented in Fig 6. These configurations are supposed to have the same geometrical parameters as considered in Section 3.1, but cladding's layers are made of Si and SiO₂. The choice of such a combination of the

constitutive media is provoked by the practical interest to the wavelength range around $1.55\text{ }\mu\text{m}$, which is a telecommunication standard.

We can see in Fig. 6 that the dispersion curves for both configurations are quite similar to each other. Thus, the dispersion parameter D is positive and reaches rather large values almost in the whole bandwidth over λ_D (here λ_D is the zero-dispersion wavelength) for both configurations. Moreover, the dispersion parameter is flattened over a relatively large wavelength range. When the dispersion curves of the corresponding mode approaches the band edges (see, Fig. 2) at large frequencies, i.e. the shortest wavelengths in Fig. 6, there are small regions with negative dispersion $D < 0$. Besides, the dispersion parameter spikes in the long wavelength limit, where $n_{eff} \rightarrow 0$ and $\beta' \rightarrow 0$.

At the same time, there are some distinctions in these dispersion curves for periodic and aperiodic configurations, which are affected by the waveguide dispersion contributions to D . Thus there is a shift of λ_D toward longer wavelengths at $\sim 100\text{ nm}$ for aperiodic configuration. Here, $\lambda_D = 1.44\text{ }\mu\text{m}$ and $\lambda_D = 1.54\text{ }\mu\text{m}$ are for Bragg reflection waveguides with periodic and aperiodic cladding, respectively. Also we can conclude that, for the waveguide with aperiodic cladding, flattened part of dispersion curve is significantly shorter, compared to the case of periodic cladding.

4. Conclusion

In conclusion, we have proposed a novel type of a planar Bragg reflection waveguide which consists of an air guiding layer sandwiched between two aperiodic mirrors which are arranged according to the Kolakoski $K(1,2)$ substitutional rule. On the basis of the transfer matrix formalism, the bandgap conditions, dispersion characteristics and mode profiles of the guided modes of such Bragg reflection waveguide are studied. Peculiarities of the dispersion properties of such Bragg reflection waveguide are investigated.

We argue that the design of cladding in the form of an aperiodic structure gives rise to changes in the waveguide dispersion, resulting in the shift of zero-dispersion point toward the longer wavelength. Besides, the flattened-dispersion region is more shorter for the waveguide with aperiodic cladding than for periodic one.

Since most of the characteristics of the planar Bragg waveguides are similar to those of the cylindrical Bragg fibers, we argue that obtained results are also applicable for prediction of optical features of the latter ones.

Acknowledgments

This work was partially supported (IAS and OVS) by University of Guanajuato (projects DAIP-633/2015 and DAIP-609/2015).